İSTANBUL UNIVERSITY CERRAHPAŞA

RESEARCH ARTICLE

Electrica 2021; 21(1): 50-57

BER Analysis For 2×2 Mimo High-Efficiency DCSK System

Nguyen Xuan Quyen

Hanoi University of Science and Technology, School of Electronics and Telecommunications, Vietnam

Cite this article as: Quyen NX. BER Analysis For 2×2 Mimo High-Efficiency DCSK System. *Electrica*, 2021; 21(1): 50-57.

ABSTRACT

This paper investigates a chaotic communication system based on the combination of high-efficiency differential-chaos-shift-keying (HEDCSK) scheme and multiple-input multiple-output technique, which aims at exploiting multi-path propagation to improve the system performance. Operation and discrete model of the system with the use of modulation/demodulation of HEDCSK and Alamouti space-time coding/decoding for 2×2 antennas are described. The bit error rate (BER) in the presence of an additive white Gaussian noise (AWGN) and Rayleigh fading is theoretically analyzed and verified by numerical simulations. Obtained results show the improvement of the BER performance of the proposed scheme compared to other related systems.
Keywords: Chaotic signals, Chaos-based communications, MIMO, DCSK, HE-DCSK, Alamouti STBC

Corresponding Author:
Nguyen Xuan Quyen

E-mail:
quyen.nguyenxuan@hust.edu.vn

Received: 11.04.2020

Accepted: 17.09.2020

DOI: 10.5152/electrica.2021.20036

Introduction

In the last decades, chaos-based communication systems have been investigated taking the advantage of chaotic waveforms [1, 2]. Owing to the given special properties, i.e., non-periodic, random-like, wideband with low cross-correlation and impulse-like auto-correlation [3, 4], chaotic signals are considered to be one of the natural candidates for spread-spectrum communications [5]. Based on the receiver's structures, chaos-based communication schemes can be broadly classified into coherent and non-coherent types [1, 2]. In the coherent schemes, a local synchronized copy of the chaotic sequence has to be produced at the receiver. As the transmitted signal is corrupted by the channel, the synchronization issue becomes very complicated [6, 7]. To avoid this issue [8], non-coherent schemes have been developed. The widely studied non-coherent schemes are mainly developed from the conventional differential-chaos-shift-keying (DCSK) scheme [9], where the demodulation and data recovery in the receiver are carried out based on the correlation characteristics of chaotic sequences [9-14]. To reduce the wasted energy for transmitting the chaotic reference, a high-efficiency DCSK (HEDCSK) scheme is proposed [15, 16]. The transmitter recycles each reference slot and two data bits are simultaneously carried in the one data-modulated sample. This scheme helps to double the bandwidth efficiency and enhance data security compared to the conventional DCSK. The BER performance of HEDCSK over AWGN and multi-path fading channels has been studied in [15] and [16], respectively. Owing to the advantages of HEDCSK, enhanced versions of this scheme have been recently developed such as frequency division multiplexing HEDCSK (FDM-HEDCSK) [17] and very high HEDCSK (VHE-DCSK) [18].

The use of multi-antenna technique, i.e., multiple-input multiple-output (MIMO), has recently been deployed widely in wireless communication systems and networks such as IEEE 802.11n (Wi-Fi), IEEE 802.11ac (Wi-Fi), HSPA+ (3G), WiMAX (4G), and Long Term Evolution (4G LTE) [19]. MIMO systems provide a robust improvement in the channel capacity, data rate, and performance. A key part of MIMO is the signal processing architecture in receivers. Among all the proposed techniques, space–time block coding (STBC) is typical and simple [20]. The STBC technique transmits multiple copies of data streams across a number of antennas to exploit various received versions for improving the communication reliability. To date, there have

been several published works studying on the combination of Alamouti STBC and non-coherent chaos-based schemes, i.e., 2×2 MIMO-DCSK [21, 22], M-ary DCSK-MIMO [23], STBC-CDSK [24], Analog STBC-DCSK [25], and so on.

Stemming from the aforementioned advantages of the HEDCSK scheme and MIMO technique, this paper proposes a combined communication system, namely 2x2 MIMO-HEDCSK, which aims to improve the capacity and performance of HEDCSK over multi-path channels. The architecture and operation of the conventional HEDCSK and proposed 2×2 MIMO-HEDCSK systems are described by means of discrete modeling. For a simplification of the mathematical analysis, BER performance is theoretically evaluated over a Gaussian noise-affected channel without considering the fading phenomenon. Numerical simulations are carried out to verify the theoretical analysis and evaluate the system performance over a Rayleigh fading channel. The obtained results show that there is a good match between the analyzed and simulated performance. In addition, there is an asymptotic performance curve which is defined as a set of minimum BER points for different cases of β and E_b/N_0. Results also prove that the proposed system can be considered to be a robust chaos-based solution for wireless communications.

The rest of the paper is structured as follows: the description of the conventional HEDCSK system is presented in Section 1, while the proposed system of 2×2 MIMO-HEDCSK is described in Section 2. The BER analysis is given in Section 3 and the comparison of the simulation results with the analytical ones is shown in Section 4. Finally, Section 5 concludes our work.

HEDCSK system

Figure 1 presents the block diagram of a conventional HEDCSK system over the AWGN [15]. Chaotic signals are generated in the form of discrete-sample sequence with chip duration

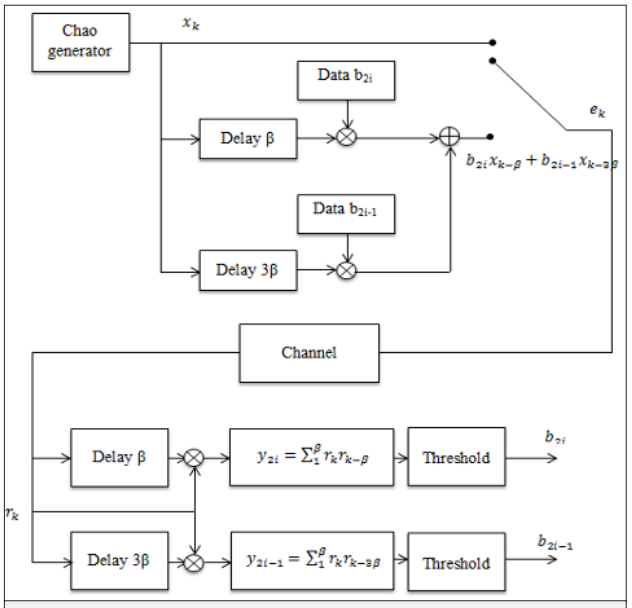

Figure 1. Block diagram of the conventional HEDCSK system [15]

in the transmitter. Each bit duration is divided into two time slots: (1) the first time slot conveys the reference chaotic sequence and (2) the second time slot conveys the sum of two bearing-data sequences. The ratio, i.e., , is the spreading factor of the system. After being delayed by the periods of and , the chaotic signals are multiplied with NRZ codes of data bits and . The sum of the resulting products is transmitted in the second slot. As a result, the transmitted signal at the output can be expressed as follows:

$$e_{i,k} = \begin{cases} x_k, 2i\beta < k \le (2i+1)\beta, \\ b_{2i}x_{k-\beta} + b_{2i-1}x_{k-3\beta}, \beta < k \le (2i+2)\beta. \end{cases} \quad (1)$$

Under the presence of the Gaussian noise from the channel, the received signal in the k^{th} chip of i^{th} bit is determined by

$$r_{i,k} = e_{i,k} + \eta_k = \begin{cases} x_k + \eta_k, 2i\beta < k \le (2i+1)\beta, \\ b_{2i}x_{k-\beta} + b_{2i-1}x_{k-3\beta} + \eta_k, (2i+1)\beta < k \le (2i+2)\beta. \end{cases} \quad (2)$$

The received signals in the second time slot are correlated with two delayed versions corresponding to the periods of and chip duration. The results can be written as

$$y_{2i} = \sum_{k=(2i+1)\beta}^{(2i+2)\beta} r_{k-\beta}r_k = \sum_{k=(2i+1)\beta}^{(2i+2)\beta} (x_{k-\beta} + \eta_{k-\beta})(b_{2i}x_{k-\beta} + b_{2i-1}x_{k-3\beta} + \eta_k), \quad (3)$$

and

$$y_{2i-1} = \sum_{k=(2i+1)\beta}^{(2i+2)\beta} r_{k-3\beta}r_k = \sum_{k=(2i+1)\beta}^{(2i+2)\beta} (x_{k-3\beta} + \eta_{k-3\beta})(b_{2i}x_{k-\beta} + b_{2i-1}x_{i-3\beta} + \eta_k). \quad (4)$$

The correlated values, y_{2i} and y_{2i-1}, are compared with zero threshold to recover the data bits, b_{2i} and b_{2i-1}, at the output.

2x2 MIMO-HEDCSK system

Figure 2 presents the block diagram of the system under study, 2×2 MIMO-HEDCSK, using Alamouti space-time block code [20]. Alamouti matrix for the i^{th} data symbols, i.e., s_1 and s_2, is defined by $S = \begin{bmatrix} s_1 & -s_2^* \\ s_2 & s_1^* \end{bmatrix}$, where * denotes complex conjugate.

Figure 2(a) and Figure 2(b) depict the schemes of the transmitter and receiver, respectively. The output signals of STBC encoder are multiplied with the delayed versions of the chaotic reference. The sum signals and chaotic reference are then transmitted on the corresponding time slot and antennas. The signals on TX antennas are determined in Table 1.

Table 1. Signal values corresponding to time slots and TX antennas

Time slot	TX1	TX2
$[0\ \beta T_c]$	X_k	X_k
$[\beta T_c\ 2\beta T_c]$	$S_1 X_{k-\beta} + S_2 X_{k-3\beta}$	$-S_2^* X_{k-\beta} + S_1^* X_{k-3\beta}$

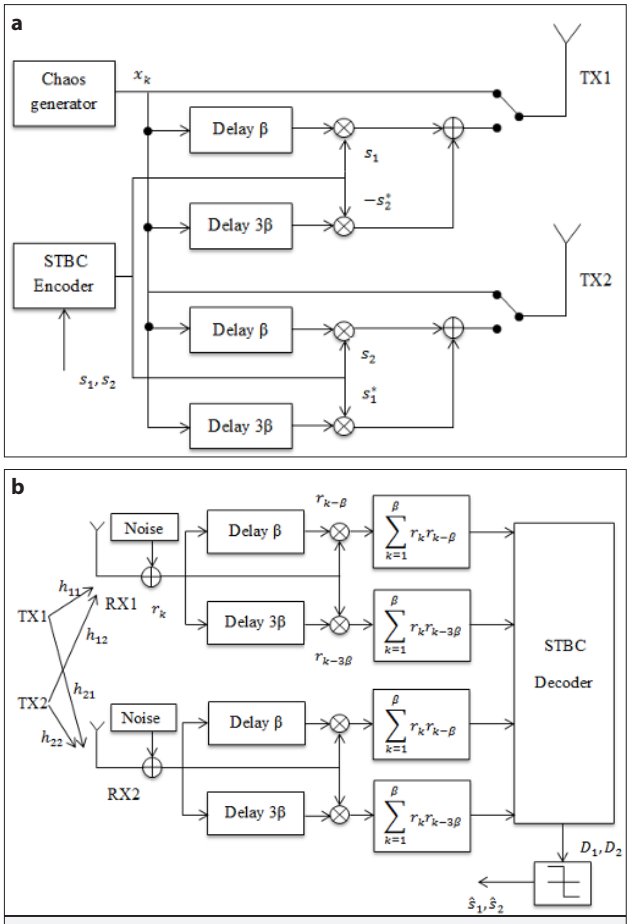

Figure 2. a, b. Block diagram of the proposed 2x2 MIMO-HEDCSK system

Table 2. Signal values corresponding to time slots and RX antennas

Receiving antenna	Time slot	Signal values
RX1	$[0\ \beta T_c]$	$h_{11}^{\square} x_k + h_{21}^{\square} x_k + \eta_k^1$
	$[\beta T_c\ 2\beta T_c]$	$h_{11}^{\square}(s_1 x_{k-\beta} + s_2 x_{k-3\beta}) + h_{21}^{\square}(-s_2^* x_{k-\beta} + s_1^* x_{k-3\beta}) + \eta_k^2$
RX2	$[0\ \beta T_c]$	$h_{12}^{\square} x_k + h_{22}^{\square} x_k + \eta_k^3$
	$[\beta T_c\ 2\beta T_c]$	$h_{12}^{\square}(s_1 x_{k-\beta} + s_2 x_{k-3\beta}) + h_{22}^{\square}(-s_2^* x_{k-\beta} + s_1^* x_{k-3\beta}) + \eta_k^4$

After going through the channels, the transmitted signals are received on the RX antennas. Table 2 represents the signal values at the corresponding time slots on the RX antennas, where $h_{11}^{\square}$, $h_{21}^{\square}$, $h_{12}^{\square}$, and $h_{22}^{\square}$ are channel coefficients for the i^{th} data symbols. The received signal on each RX antenna is simultaneously correlated with its delayed versions in the second time slot. There are four correlators that are totally equivalent to each other. Therefore, for simplifying the mathematical expression, we just consider the correlation value at the output of the first one, which is

$$\begin{aligned} y_{11} &= T_c \sum_{k=1}^{\beta} r_k r_{k-\beta} \\ &= T_c \sum_{k=1}^{\beta} \begin{pmatrix} h_{11}^{\square}(s_1 x_{k-\beta} + s_2 x_{k-3\beta}) \\ +h_{21}^{\square}(-s_2^* x_{k-\beta} + s_1^* x_{k-3\beta}) + \eta_k^2 \\ (h_{11}^{\square} x_{k-\beta} + h_{21}^{\square} x_{k-\beta} + \eta_k^1) \end{pmatrix} \\ &= T_c \sum_{k=1}^{\beta} x_{k-\beta}^2 (h_{11}^{\square} s_1 - h_{21}^{\square} s_2^*)(h_{11}^{\square} + h_{21}^{\square}) \\ &+ T_c \sum_{k=1}^{\beta} x_{k-\beta} x_{k-3\beta} (h_{11}^{\square} s_2 + h_{21}^{\square} s_1^*)(h_{11}^{\square} + h_{21}^{\square}) \\ &+ T_c \sum_{k=1}^{\beta} \begin{pmatrix} \eta_k^1 x_{k-\beta}(h_{11}^{\square} s_1 - h_{21}^{\square} s_2^*) \\ +\eta_k^1 x_{k-3\beta}(h_{11}^{\square} s_2 + h_{21}^{\square} s_1^*) \\ +\eta_k^2 x_{k-\beta}(h_{11}^{\square} + h_{21}^{\square}) + \eta_k^2 \eta_k^1 \end{pmatrix}. \end{aligned} \tag{5}$$

In the proposed system, each transmitted symbol consists of a chaotic reference slot and a data-bearing slot. The energy of the data-bearing slot doubles that of the reference one, hence, the bit energy can be calculated by

$$Eb = \tfrac{3}{2} \sum_{k=1}^{\beta} x_k^2. \tag{6}$$

Based on Eq. (5), the equivalent baseband model of the received symbol on the antenna RX1 within $[0\ \beta T_c]$ is

$$Y_{11} = \frac{y_{11}}{h_{11}^{\square} + h_{21}^{\square}} = \frac{2}{3} Eb\left(h_{11}^{\square} s_1 - h_{21}^{\square} s_2^*\right) + \phi_{11} + \psi_{11}, \tag{7}$$

where ϕ_{11} is the inter-symbol interference (ISI) component given by

$$\phi_{11} = \sum_{k=1}^{\beta} x_{k-\beta} x_{k-3\beta} \left(h_{11}^{\square} s_2 + h_{21}^{\square} s_1^*\right), \tag{8}$$

and is Gaussian noise component, i.e.,

$$\begin{aligned} \psi_{11} &= \sum_{k=1}^{\beta} \eta_k^1 x_{k-\beta} \frac{h_{11}^{\square} s_1 - h_{21}^{\square} s_2^*}{h_{11}^i + h_{21}^i} \\ &+ \sum_{k=1}^{\beta} \eta_k^1 x_{k-3\beta} \frac{(h_{11}^{\square} s_2 + h_{21}^{\square} s_1^*)}{h_{11}^i + h_{21}^i} \\ &+ \sum_{k=1}^{\beta} \eta_k^2 x_{k-\beta} + \sum_{k=1}^{\beta} \frac{1}{h_{11}^{\square} + h_{21}^{\square}} \eta_k^2 \eta_k^1. \end{aligned} \tag{9}$$

Similarly, the received symbol on the antenna RX1 within $[\beta T_c, 2\beta T_c]$ is determined as

$$Y_{21} = \frac{y_{21}}{h_{11}^{\square} + h_{21}^{\square}} = \frac{2}{3} Eb\left(h_{11}^{\square} s_2 + h_{21}^{\square} s_1^*\right) + \phi_{21} + \psi_{21}, \tag{10}$$

with the ISI and noise-affected components being

$$\phi_{21} = \sum_{k=1}^{\beta} x_{k-\beta} x_{k-3\beta} \left(h_{11}^{\square} s_1 - h_{21}^{\square} s_2^*\right), \tag{11}$$

and

$$\psi_{21} = \sum_{k=1}^{\beta} \eta_{k-3\beta}^{1} x_{k-\beta} \frac{h_{11}^{\square} s_1 - h_{21}^{\square} s_2^*}{h_{11}^{\square} + h_{21}^{\square}} + \sum_{k=1}^{\beta} \eta_{k-3\beta}^{1} x_{k-3\beta} \frac{(h_{11}^{\square} s_2 + h_{21}^{\square} s_1^*)}{h_{11}^{\square} + h_{21}^{\square}} + \sum_{k=1}^{\beta} \eta_{k-3\beta}^{2} x_{k-3\beta} + \sum_{k=1}^{\beta} \frac{1}{h_{11}^{\square} + h_{21}^{\square}} \eta_k^2 \eta_{k-3\beta}^{1}. \quad (12)$$

Carring out the analysis in the same way, the received symbols, Y_{12} and Y_{22} on the antenna RX2 are expressed by

$$\begin{bmatrix} Y_{11} \\ Y_{12} \\ Y_{21} \\ Y_{22} \end{bmatrix} = \frac{2}{3} Eb \begin{bmatrix} h_{11}^{\square} s_1 - h_{21}^{\square} s_2^* \\ h_{12}^{\square} s_1 - h_{22}^{\square} s_2^* \\ h_{21}^{\square} s_1^* + h_{11}^{\square} s_2 \\ h_{22}^{\square} s_1^* + h_{12}^{\square} s_2 \end{bmatrix} + \begin{bmatrix} \phi_{11} \\ \phi_{12} \\ \phi_{21} \\ \phi_{22} \end{bmatrix} + \begin{bmatrix} \psi_{11} \\ \psi_{12} \\ \psi_{21} \\ \psi_{22} \end{bmatrix}. \quad (13)$$

In the analysis, the data symbols are assumed to be real values. Thus, $s_1=s_1^*$, $s_2=s_2^*$, and Eq. (13) becomes

$$\begin{bmatrix} Y_{11} \\ Y_{12} \\ Y_{21} \\ Y_{22} \end{bmatrix} = \frac{2}{3} Eb \begin{bmatrix} h_{11}^{\square} & -h_{21}^{\square} \\ h_{12}^{\square} & -h_{22}^{\square} \\ h_{21}^{\square} & h_{11}^{\square} \\ h_{22}^{\square} & h_{12}^{\square} \end{bmatrix} \begin{bmatrix} s_1 \\ s_2 \end{bmatrix} + \begin{bmatrix} \phi_{11} \\ \phi_{12} \\ \phi_{21} \\ \phi_{22} \end{bmatrix} + \begin{bmatrix} \psi_{11} \\ \psi_{12} \\ \psi_{21} \\ \psi_{22} \end{bmatrix}, \quad (14)$$

which can be written in a short form as

$$Y = \mathrm{HS} + \phi + \psi. \quad (15)$$

To determine the data bits, the matrix Y is multiplied with the conjugate transpose H^T of the channel matrix H as shown below.

$$\begin{bmatrix} \mathrm{D}_1 \\ \mathrm{D}_2 \end{bmatrix} = \mathrm{H^T Y} = \begin{bmatrix} \mathrm{h}_{11}^{\square} & \mathrm{h}_{12}^{\square} & \mathrm{h}_{21}^{\square} & \mathrm{h}_{22}^{\square} \\ -\mathrm{h}_{21}^{\square} & -\mathrm{h}_{22}^{\square} & \mathrm{h}_{11}^{\square} & \mathrm{h}_{12}^{\square} \end{bmatrix} \begin{bmatrix} \mathrm{Y}_{11} \\ \mathrm{Y}_{12} \\ \mathrm{Y}_{21} \\ \mathrm{Y}_{22} \end{bmatrix} = \frac{2}{3} \mathrm{EbH^T H} + \mathrm{H^T}\phi + \mathrm{H^T}\psi. \quad (16)$$

By this way, decision variables D_1 and D_2 are calculated as follows:

$$D_1 = \frac{2}{3} Eb \sum_{m,n=1}^{2} \left(h_{mn}^{\square}\right)^2 s_1 + \left(h_{11}^{\square}\phi_{11} + h_{12}^{\square}\phi_{12} + h_{21}^{\square}\phi_{21} + h_{22}^{\square}\phi_{22}\right) + \left(h_{11}^{\square}\psi_{11} + h_{12}^{\square}\psi_{12} + h_{21}^{\square}\psi_{21} + h_{22}^{\square}\psi_{22}\right), \quad (17)$$

$$D_2 = \frac{2}{3} Eb \sum_{m,n=1}^{2} \left(h_{mn}^{\square}\right)^2 s_2 + \left(h_{11}^{\square}\phi_{21} + h_{12}^{\square}\phi_{22} - h_{21}^{\square}\phi_{11} - h_{22}^{\square}\phi_{12}\right) + \left(h_{11}^{\square}\psi_{21} + h_{12}^{\square}\psi_{22} - h_{21}^{\square}\psi_{11} - h_{22}^{\square}\psi_{12}\right). \quad (18)$$

The data bits are finally recovered by

$$\hat{\mathrm{s}}_1 = \begin{cases} 1, \mathrm{D}_1 > 0, \\ 0, \mathrm{D}_1 \le 0, \end{cases} \quad (19)$$

$$\hat{\mathrm{s}}_2 = \begin{cases} 1, \mathrm{D}_2 > 0, \\ 0, \mathrm{D}_2 \le 0. \end{cases} \quad (20)$$

BER Analysis over AWGN channel

To simplify the BER analysis and mathematical expression, the performance of the 2x2 MIMO-HEDCSK system is theoretically evaluated under the following assumptions: (i) Data symbols, s_1 or s_2, are real binary numbers with either "+1" or "−1" appearing at the output of the data source with the same probability; (ii) The channel is only affected by the Gaussian noise. It means that the values of fading coefficients described in Section 3 are equal to 1, i.e., $h_{m,n}=1$ for m, $n=1\div2$. Due to the equivalence of statistical characteristics of D_1 and D_2 and under the assumptions above, the variable D_1 can be represented by

$$D_1 = U + I + N, \quad (21)$$

where U, I, and N are the beneficial information, ISI, and noise-affected components, respectively, which are given as

$$U = \frac{8}{3} E_b, \quad (22)$$

$$I = 4 \sum_{k=1}^{\beta} x_{k-\beta} x_{k-3\beta}, \quad (23)$$

$$N = \sum_{k=1}^{\beta} \eta_k^1 x_{k-3\beta} + \sum_{k=1}^{\beta} \eta_k^2 x_{k-\beta} + \frac{1}{2} \sum_{k=1}^{\beta} \eta_k^2 \eta_k^1. \quad (24)$$

For the generation of chaotic sequences, the system uses the 2nd-order polynomial Chebysev function, i.e., $x_{k+1} = 2x_k^2 - 1$, with the mean values of $E[x_k]$ and $E[x_k^2] = 0.5$ [26]. Suppose that the value β is large enough so that the correlation values of the independent elements, I and N, are approximate to zero. The average value of D_1 can be calculated as

$$E[D_1] = E[U] + E[I] + E[N] = \frac{8}{3} E_b + 4E\left[\sum_{k=1}^{\beta} x_{k-\beta} x_{k-3\beta}\right] + E\left[\sum_{k=1}^{\beta} \eta_k^1 x_{k-3\beta}\right] + E\left[\sum_{k=1}^{\beta} \eta_k^2 x_{k-\beta}\right] + \frac{1}{2} E\left[\sum_{k=1}^{\beta} \eta_k^2 \eta_k^1\right] = \frac{8}{3} E_b. \quad (25)$$

Next, the variance of D_1 is determined by

$$Var[D_1^{\square}] = Var[U] + Var[I] + Var[N]$$

$$E_b + 16E\left[\left(\sum_{k=1} x_{k-\beta} x_{k-3\beta}\right)\right] + E\left[\left(\sum_{k=1}^{\beta} \eta_k^1 x_{k-3\beta}\right)^2\right] + E\left[\left(\sum_{k=1}^{\beta} \eta_k^2 x_{k-\beta}\right)\right] \cdot \frac{1}{4} E\left[\left(\sum_{k=1}^{\beta} \eta_k^2 \eta_k^1\right)^2\right] = \frac{16}{3} E_b + \frac{8}{3} E_b N_0 + \frac{\beta}{} \quad (26)$$

Since the statistical numbers of the decisive variable D1 in all the cases of s_1 and s_2 are equal, based on Eq. (25) and Eq. (26), the BER equation can be rewritten as:

$$BER = Q\left(\left(\frac{Var[D_1]}{E[D_1]^2}\right)^{-0.5}\right) = Q\left(\left(\frac{Var[D_2]}{E[D_2]^2}\right)^{-0.5}\right)$$
$$= Q\left(\left(\frac{\frac{16}{3}E_b + \frac{8}{3}E_bN_0 + \frac{\beta N_0^2}{4}}{\left(\frac{8E_b}{3}\right)^2}\right)^{-0.5}\right)$$
$$= Q\left(\left(\frac{3}{4E_b} + \frac{3}{8\frac{E_b}{N_0}} + \frac{9\beta}{256\left(\frac{E_b}{N_0}\right)^2}\right)^{-0.5}\right), \quad (27)$$

with the Q function defined as $Q(e) = \frac{1}{2\pi}\int_e^{\infty} exp\left(\frac{y^2}{2}\right)dy$ [27].

Let us consider the elements within the brackets of Eq. (27). For a fixed value of β, BER value is inversely proportional to the ratio E_b/N_0. In the case of the ratio E_b/N_0 being fixed, the increment of β leads to the decrement of both 1st element, $\frac{3}{4E_b}$, and the increment of 3rd element, $\frac{9\beta}{256\left(\frac{E_b}{N_0}\right)^2}$, and vice versa. It means that for each fixed value of $\frac{E_b}{N_0}$, there is always a corresponding optimal value of β, i.e., $\beta_{opt} = \frac{16}{3}\frac{E_b}{N_0}$, at which happening, $\frac{3}{4E_b} = \frac{9\beta_{Opt}}{256\left(\frac{E_b}{N_0}\right)^2}$, and the system achieves a minimum BER. Based on Eq. (27), the minimum BER value at β_{Opt} can be determined by

$$BER_{Min} = Q\left(\left(\frac{3}{4\frac{E_b}{N_0}}\right)^{-0.5}\right), \quad (28)$$

which can be considered to be the asymptotic BER of 2x2 MIMO-HEDCSK system.

Simulation results

In this section, a Monte Carlo simulation is carried out and the simulated results are shown to verify the theoretical performance obtained by the above analysis.

BER performance of MIMO-HE-DCSK by means of both the theoretical analysis and numerical simulation in the cases of β=10, β=50, and β=100 are presented in Figure 3. A good match is observed between the analyzed and simulated results for all different values of E_b/N_0 and spreading factor. For the ratio E_b/N_0 less than 7.5dB, the BER performance gets better when the value of β increases from 10 to 100. In contrast, with E_b/N_0 greater than 7.5dB, the system in the cases of β=10 and β=50 performs worst and best, respectively.

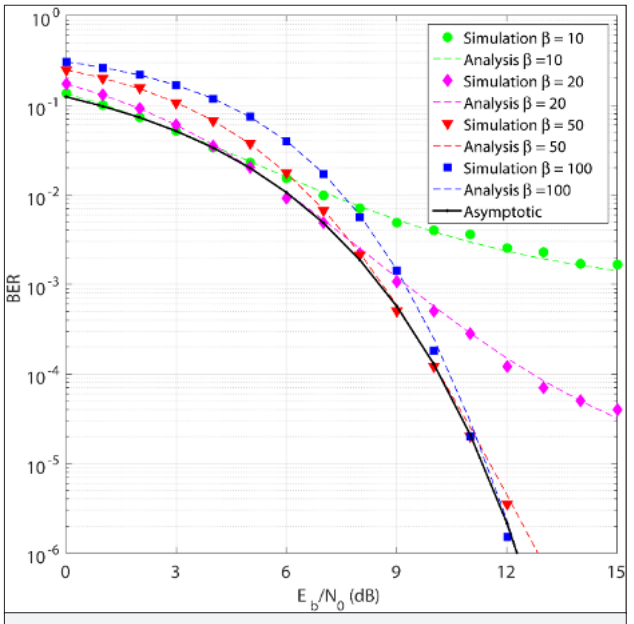

Figure 3. BER versus E_b/N_0 with diffirent values of spreading factor

To elaborate the dependence of system performance on the spreading factor, Figure 4 presents the theoretical and numerical BER curves versus β in the cases of E_b/N_0=3*dB*, 7*dB*, and 9*dB*. It clearly appears that in the value range of β from 40 to 140, the increment of β increases the BER values. BERs in the cases of E_b/N_0=3*dB*, 7*dB*, and 9*dB* are found to achieve their minimum values at β=10, 27, and 42, respectively. These results verify the asymptotic behavior of the system determined by Eq. (28). In particular, good performance is obtained for low spreading

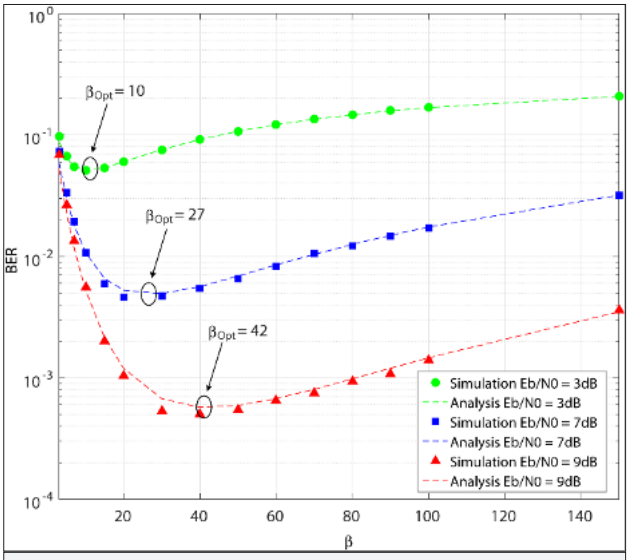

Figure 4. BER versus the spreading factor with diffirent values of E_b/N_0

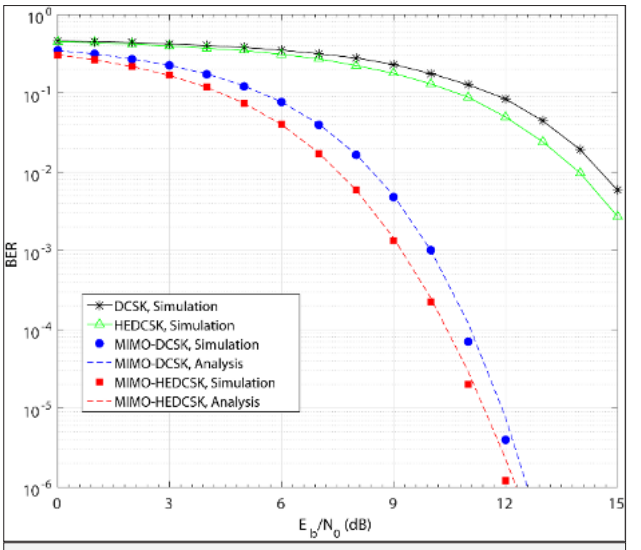

Figure 5. BER comparison over AWGN channel between DCSK [9], HEDCSK [15], 2x2 MIMO-DCSK [22], and 2x2 MIMO-HEDCSK

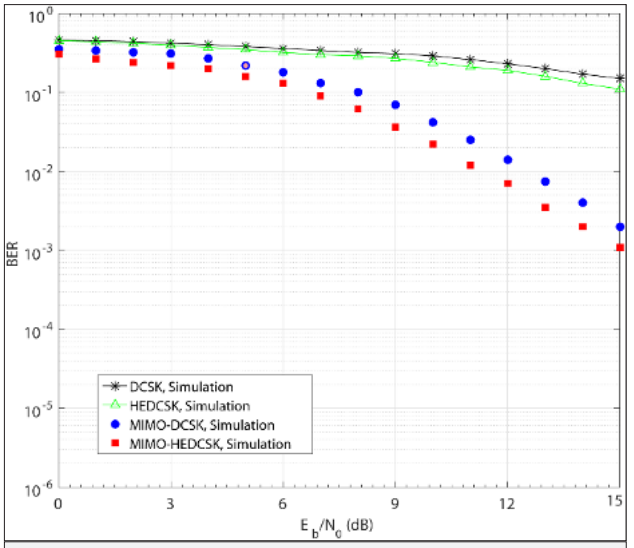

Figure 6. BER comparison over Rayleigh channel between DCSK [1], [9], HEDCSK [15], [16], 2x2 MIMO-DCSK [22], and 2x2 MIMO-HEDCSK

factor values, making this system implementation feasible even for a moderate bandwidth.

A comparison of the simulated BER of the 2x2 MIMO-HEDCSK in the case of β=100 with those of the conventional DCSK, HEDCSK and MIMO-DCSK over AWGN and Rayleigh flat-fading channel are shown in Figure 5 and Figure 6, respectively. The fading-affected performance is numerically evaluated under the condition of fading coefficients, i.e., $E[h_{11}^2] = E[h_{12}^2] = E[h_{21}^2] = E[h_{22}^2] = 1$. It is evident that the BER performance of the proposed systems is significantly better than those of the remaining systems. For example, at the same E_b/N_0=12dB, the BER values of DCSK, HEDCSK, MIMO-DCSK, and 2x2 MIMO-HEDCSK over AWGN and Rayleigh fading channels respectively correspond to $9.1 \cdot 10^{-2}$, $4.2 \cdot 10^{-6}$, $1.2 \cdot 10^{-6}$, and $2.1 \cdot 10^{-1}$, $1.8 \cdot 10^{-1}$, $1.4 \cdot 10^{-2}$, $7.2 \cdot 10^{-3}$.

Conclusion

In this paper, a communication scheme for wireless applications that combines the 2×2 MIMO technique and HEDCSK scheme is studied. The operation and signal processing in the transmitter and receiver is described in detail. The BER performance over the AWGN and Rayleigh fading channels is theoretically analyzed and verified by Monte Carlo simulations. Obtained results showed that the 2×2 MIMO-HEDCSK system can take advantage of the multipath and multiple-antenna propagation in radio communications to improve the BER performance compared with other related schemes. Although the proposed system is somewhat more complex compared to others, it is still really practical considering the advanced development of CMOS technology and the freedom from synchronization in the proposed scheme of this study.

Peer-review: Externally peer-reviewed.

Conflict of Interest: The author has no conflicts of interest to declare.

Financial Disclosure: The author declared that the study has received no financial support.

References

1. F. Lau, C. Tse, "Chaos-based Digital Communication Systems: Operating Principles, Analysis Methods, and Performance Evaluation", Springer, 2003.
2. W. Tam, F. Lau, C. Tse, "Digital Communications with Chaos: Multiple Access Techniques and Performance", Elsevier Science, 2006.
3. N. X. Quyen, Y. V. Vu, T. D. Nguyen, B. T. Quyet, "Simulation and implementation of improved chaotic Colpitts circuit for UWB communications", in 3rd Int. Conf. on Commun. and Elect., Nha Trang, Vietnam, 2010, pp. 307-312.
4. J. Yu, Y.-D. Yao, "Detection performance of chaotic spreading LPI waveforms", IEEE Trans. Wireless Comm., vol. 4, no. 2, pp. 390-396, 2005. [CrossRef]
5. G. Kaddoum, "Wireless chaos-based communication systems: a comprehensive survey", IEEE Access, vol. 4, 2016. 2621-2648. [CrossRef]
6. N. X. Quyen, T. Q. Duong, N. Vo, Q. Xie, L. Shu, "Chaotic direct-sequence spread-spectrum with variable symbol period: A technique for enhancing physical layer security", Computer Networks, vol. 109, pp. 4-12, 2006. [CrossRef]
7. S. M. Berber, A. K. Gandhi, "Inherent diversity combining techniques to mitigate frequency selective fading in chaos-based DSSS systems", Physical Communication, vol. 19, pp. 30-37, 2016. [CrossRef]
8. S. M. Berber, "Discrete time domain analysis of chaos-based wireless communication systems with imperfect sequence synchronization", Signal Processing, vol. 154, pp. 198-206, 2019. [CrossRef]
9. G. Kolumbán, B. Vizvari, W. Schwarz, A. Abel, "Differential chaos shift keying: a robust code for chaos communication", in 4th Int. Workshop on Nonlinear Dynamics Elect. Syst., 1996, pp. 87-92.
10. G. Kaddoum, E. Soujeri, C. Arcila, K. Eshteiwi, "I-DCSK: An improved noncoherent communication system architecture", IEEE Trans. Circuits Syst. II, Exp. Briefs, vol. 62, no. 9, pp. 901-905, 2015. [CrossRef]
11. M. Herceg, D. Vranješ, G. Kaddoum, E. Soujeri, "Commutation code index DCSK modulation technique for high-data-rate communication systems", IEEE Trans Circuits Syst II Express Briefs, vol. 65, no. 12, pp. 1954-1958, 2018. [CrossRef]
12. G. Cheng, X. Chen, W. Liu, W. Xiao, "GCI-DCSK: Generalized Carrier Index Differential Chaos Shift Keying Modulation", IEEE Commun Lett, vol. 23, no. 11, pp. 2012-2016, 2019. [CrossRef]
13. G. Cai, Y. Fang, J. Wen, S. Mumtaz, Y. Song, V. Frascolla, "Multi-Carrier M-ary DCSK System With Code Index Modulation: An Efficient Solution for Chaotic Communications", IEEE J Sel Top Signal Process, vol. 13, no. 6, pp. 1375 - 1386, 2019. [CrossRef]
14. N. X. Quyen, "Quadrature MC-DCSK scheme for chaos-based cognitive radio", Int J Bifurcat Chaos, vol. 29, no. 13, p. 1950177, 2019. [CrossRef]
15. H. Yang, G-P. Jiang, "High-Efficiency Differential-Chaos-Shift-Keying Scheme for Chaos-Based Noncoherent Communication", IEEE Trans Circuits Syst I Regul Pap, vol. 59, no. 5, pp. 312-316, 2012. [CrossRef]
16. N. X. Quyen, "Bit-error-rate evaluation of high-efficiency differential-chaos-shift-keying system over wireless channels", Journal of Circuits, Systems and Computers, vol. 27, no. 01, p.1850008, 2018. [CrossRef]
17. W. Shaonan, L. Yingjie, M. Weijiao, "Design of a novel frequency division scheme for DCSK chaos communication system", 3rd Int.

Conf. on Information Management (ICIM), Chengdu, 2017, pp. 317-321. [CrossRef]

18. F. Taleb, F. T. Bendimerad, D. Roviras, "Very high efficiency differential chaos shift keying system", IET Communications, vol. 10, no. 17, pp. 2300-2307, 2016. [CrossRef]
19. E. G. Larsson, O. Edfors, F. Tufvesson, T. L. Marzetta, "Massive MIMO for next generation wireless systems", IEEE Communications Magazine, vol. 52, no. 2, pp. 186-195, 2014. [CrossRef]
20. H. Lipfert, "MIMO OFDM Space Time Coding - Spatial Multiplexing, Increasing Performance and Spectral Efficiency in Wireless Systems", Part I Technical Basis (Technical report). Institut für Rundfunktechnik, 2007.
21. H. F. Ma, H. B. Kan, "Space-time coding and processing with differential chaos shift keying scheme", IEEE Int. Commun. Conf. (ICC), Dresden, Germany, 2009, pp. 1-5.
22. G. Kaddoum, M. Vu, F. Gagnon, "Performance analysis of differential chaotic shift keying communications in MIMO systems", in 2011 IEEE Int. Symp. of Circuits and Systems (ISCAS), Rio de Janeiro, 2011, pp. 1580-1583. [CrossRef]
23. S. Wang, X. Wang, "M-DCSK-Based Chaotic Communications in MIMO Multipath Channels with No Channel State Information", IEEE Trans Circuits Syst II Express Briefs, vol. 57, no. 12, pp. 1001-1005, 2010. [CrossRef]
24. J. Lee, H. Ryu, "Diversity method in the chaos CDSK communication system", 16th Int. Conf. on Advanced Communication Technology, PyeongChang, 2014, pp. 1184-1187. [CrossRef]
25. P. Chen, L. Wang, F. C. M. Lau, "One Analog STBC-DCSK Transmission Scheme not Requiring Channel State Information", IEEE Trans. on Circuits and Systems I: Regular Papers, vol. 60, no. 4, pp. 1027-1037, 2013. [CrossRef]
26. T. Geisel, V. Fairen, "Statistical properties of chaos in Chebyshev maps", Phys. Lett. A., vol. 105A, pp. 263-266, 1984. [CrossRef]
27. P. Borjesson, C.-E. Sundberg, "Simple Approximations of the Error Function Q(x) for Communications Applications", IEEE Transactions on Communications, vol. 27, no. 3, pp. 639-643, 1979. [CrossRef]

Nguyen Xuan Quyen received the Diploma of Engineer, Master and PhD degrees in Electronics and Telecommunications in 2006, 2008 and 2013, respectively. From 2007 to current, he has been serving as senior lecturer at School of Electronics and Telecommunications (SET), Hanoi University of Science and Technology (HUST), Vietnam. He was sandwich PhD student at the Institute for Smart System Technologies, Alpen-Adria Klagenfurt University, Austria during 2011-2012. During 2014-2015, he has worked as a postdoctoral researcher at Department of Computer Architecture, Polytechnic University of Catalonia (UPC BarcelonaTech), Barcelona, Spain. He was also the academic visitor at the Department of Electronic and Computer Engineering, University of Limerick, Ireland in 2015, at School of Electronics, Electrical Engineering and Computer Science, Queen's University Belfast, United Kingdom in 2016, and at Department of Computer and Network Engineering, The University of Electro-Communications, Tokyo-Japan in 2017. He has been qualified with the title of associate professor at SET-HUST since 2018. His main research interests are microwave engineering, chaos-based digital communications and physical layer security, and wireless communications.